

# The Antares Emission Nebula and Mass Loss of $\alpha$ Sco A

Dieter Reimers, Hans-Jürgen Hagen,  
Robert Baade, Kilian Braun  
(all Hamburger Sternwarte, Universität  
Hamburg, Germany)

The Antares nebula has been known as a peculiar [Fe II] emission nebula, apparently without normal H II region lines. Long-slit VLT/UVES mapping shows that it is an H II region 3" in size around the B type star  $\alpha$  Sco B, with a Balmer line recombination spectrum and [N II] lines, but no [O II] and [O III]. The reason for the non-visibility of [O II] is the low electron temperature of 4900 K, while [N II] is seen because the nitrogen abundance is enhanced by a factor of three due to the CNO cycle. We derive a mass-loss rate of  $1.05 \pm 0.3 \times 10^{-6} M_{\odot}/\text{yr}$  for the M supergiant  $\alpha$  Sco A. The [Fe II] lines seem to come mainly from the edges of the H II region.

## An iron rich nebula?

The story of the Antares nebula began in 1937 with the finding of O. C. Wilson and R. F. Sanford at the Mount Wilson Observatory that the spectrum of the B-type companion of Antares, itself an M supergiant, showed forbidden emission lines of Fe II. Later Otto Struve showed that the [Fe II] lines extend  $\sim 2''$  beyond the seeing disc of the B star. Struve & Zeberg (1962) describe extensively the Antares nebula and conclude: "It is strange that the nebulosity around the B type component shows only emission lines of iron and silicon, but not those of hydrogen. The enormous abundance of hydrogen in all known gaseous nebulae and the conditions of excitation and ionization resulting from the radiation of a B type star would render it almost inexplicable for a gas of normal composition to show only the iron and silicon lines in emission. This gave rise to the hypothesis that the material in the vicinity of Antares is metal rich, in turn leading to the supposition that the envelope may be composed of solid substances such as meteors that have become vaporized and are excited by the radiation of the hot B star. This hypothesis is admittedly improbable and may have to be abandoned in the light of future work." We may add here that the mystery has lasted 45 years until, with

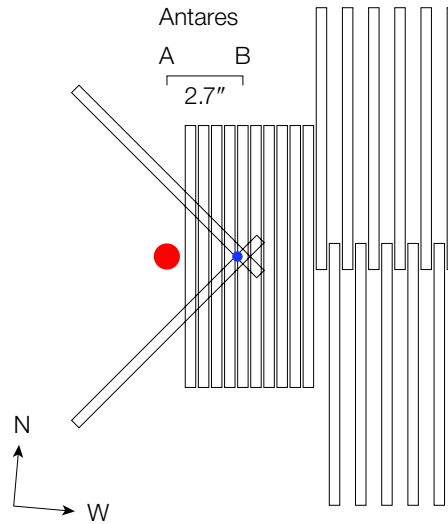


Figure 1. Geometry of the Antares system together with the UVES spectrograph slit sizes and positions shown to scale.

UVES/VLT spectra, the Antares nebula puzzle could be solved.

The most extensive previous study was that by Swings & Preston (1978) based on high-resolution long-slit photographic spectra taken with the Mt. Wilson 100" and Palomar 200" telescopes. They found that the '[Fe II] rich nebula' is strong roughly 3.5" around the B star and is surrounded by a zone of weaker lines which may extend in a NW-SE direction up to 15". However, they neither observed Balmer recombination lines nor any classical H II region lines from ions like O II, O III, S II, and N II. Therefore the nature of the Antares nebula could not be understood. In a first quantitative study of the Antares system it could be shown that the B star creates an H II region within the wind of  $\alpha$  Sco A and that the [Fe II] lines must be formed in this H II region (Kudritzki & Reimers, 1978). Later the H II region was detected as an optically thin radio emitter with a diameter of  $\sim 3''$  (Hjellming & Newell, 1983).

## UVES 2-D spectroscopy

With the construction and operation of UVES at the VLT it was obvious that progress in our understanding of the kinematics of the Antares nebula should be possible with its high spectral resolution and high pointing accuracy, making pos-

sible a 2-D mapping of the nebula with long-slit spectroscopy. We used UVES with a 0.4" slit and a resolution of 80 000 and covered the nebula with 23 long-slit positions (Figure 1). Exposure times were between 50 and 100 s (the Antares nebula is bright!); the typical seeing was 0.6" which means that the angular resolution corresponds roughly to the slit steps as shown in Figure 1.

Quite unexpected was that all spectra – even 10" from the M supergiant – are completely corrupted by scattered light from the M supergiant. This was a surprise, also to the UVES team at ESO. ESO finally made a test placing the UVES slit 10" from a bright star – with the same result as in our spectra. Apparently, light from the bright star is scattered by the slit jaws back to the slit viewing camera and from there again into the spectrograph slit. This should be a warning for anybody using UVES on faint targets close to bright sources, e.g. a disc, around a bright star.

Did this mean that our spectra were useless? It meant that, due to the ubiquitous scattered light, no general background reduction was possible and no absolute line fluxes could be deduced. Data reduction required an enormous load of extra work. In brief, the scaled M star spectrum was used as a background template. The template was fitted to the spectrum – allowing for an offset and a scaling – outside a region of  $\pm 30$  km/s of each detected emission line and was finally subtracted from the data.

The final results after this elaborate data reduction – each of the roughly 90 detected emission lines had to be treated individually in each of the spectra – are 2-D brightness distributions (location on the slit versus velocity) as a function of the location relative to the M supergiant, as shown for the H $\alpha$  line in Figure 2 and for [Fe II] 4814.55 Å in Figure 3.

## A peculiar H II region?

The main puzzle of the Antares Nebula has been resolved by our UVES data. The Balmer recombination lines expected for an H II region: H $\alpha$ , H $\beta$  ... up to H10 are present, and their geometrical extent on the sky is virtually identical to that of

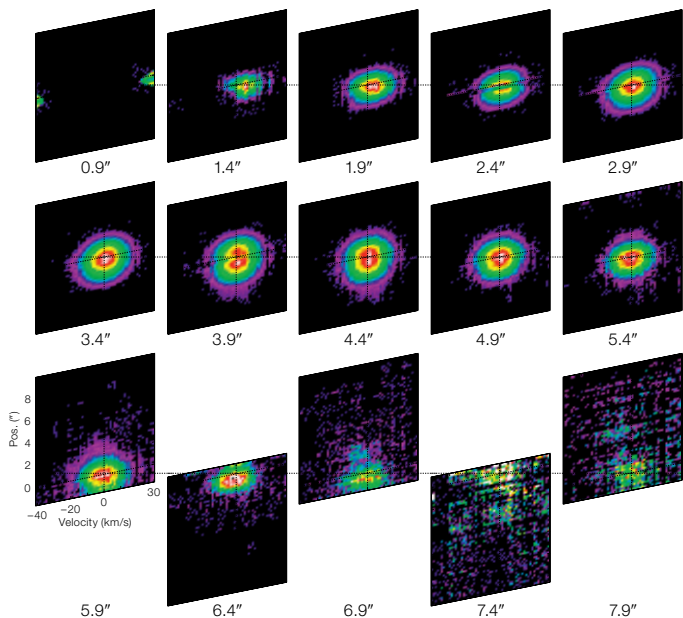


**Figure 2.**  $H\alpha$  2-D brightness distributions (location on the slit versus velocity) as a function of spectrograph slit position relative to  $\alpha$  Sco A. Offsets from the position of  $\alpha$  Sco A are shown in arcsec. Notice that due to the M star wind expansion, the velocity coordinate corresponds to the spatial depth (perpendicular to the plane of the sky). The density in the plots has been rescaled in order to provide maximum visibility. The true line fluxes vary by a factor of 150 between 1.9" and 7.9".

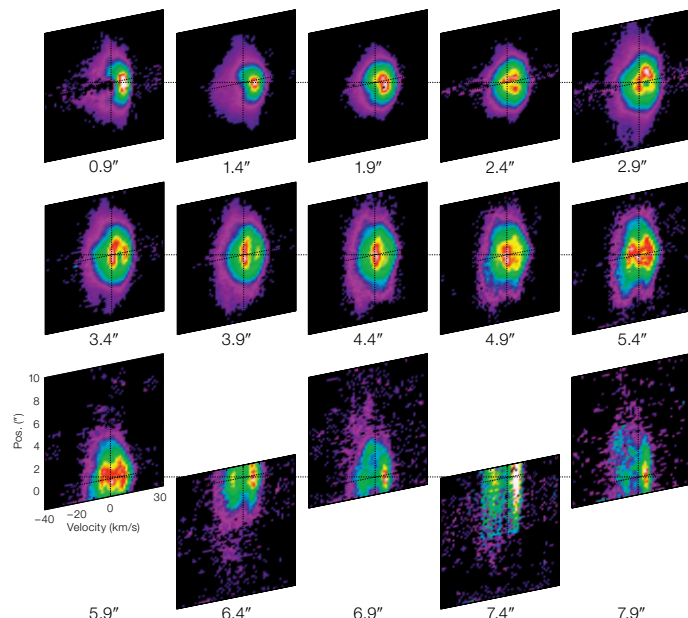


**Figure 3.**  $[Fe II]$  4814.55 Å 2-D brightness distributions as a function of spectrograph slit position (see caption of Figure 2). Notice the double structure is probably formed by the front (blueshifted) and rear (redshifted) edges of the  $H II$  region carried by the wind to large distances from the system.

the radio emission seen with the VLA (Figure 4). So why have previous observations not shown the hydrogen lines? The reason is probably that the strongest lines  $H\alpha$  and  $H\beta$  suffered, in the Mt. Wilson and Mt. Palomar photographic spectra, from seeing-dominated contamination by the M supergiant and the signal-to-noise of the photographic spectra was never sufficient to enable an efficient background subtraction.

The strongest lines are of  $[Fe II]$  such as 4287.4 Å, 4359.34 Å and 4814.55 Å. Altogether we have identified some 90 emission lines, besides  $[Fe II]$  a few  $[N II]$  and several strong allowed  $Fe II$  lines like 3177.53 Å and 4923.9/5018.4/5169.0 Å (see below). Besides the  $Si II$  lines 3856 and 3862 Å we have detected further  $S III$  lines around 5050 Å and at 6347/6371 Å (for details and a line list cf. Reimers et al., 2008).

In all previous investigations of the Antares nebula the question remained open why the 'classical' emission lines

normally prominent in  $H II$  region spectra like  $[O III]$  4959/5007 Å,  $[O II]$  3726/3729 Å,  $[N II]$  6583/6548 Å and  $[S II]$  6716/6731 Å had not been detected. Our UVES spectra allow a more critical assessment than earlier photographic spectra. The answer is that we do see faint  $[N II]$  6583 Å and 6548 Å lines, and that none of the other lines is present.  $[N II]$  6583 Å follows closely the  $H\alpha$  distribution on the sky shown in Figure 2. Since it is close to  $H\alpha$ , we can measure the  $H\alpha/[N II]$  6583.4 Å ratio as a function of the location in the nebula. Close to the B star – in the middle of the  $H II$  region –  $H\alpha/[N II] \approx 3.5$  while 3" west of B, at the outer edge of the  $H II$  region, it is  $\sim 10$ .

For  $[O II]$  we can give an upper limit: we have detected the Balmer line series up to  $H_{10}$ , but  $H_{11}$  (close to  $[O II]$  3726/3729) was not visible. Thus, the  $H_{10}$  intensity as predicted by recombination theory, can be regarded as an upper limit to  $[O II]$  which yields  $[O II]/H\alpha < 0.017$  for 3726 Å. So why is  $[N II]$  present, while the lines of  $[O II]$  and  $[O III]$ , usually stronger in  $H II$

regions, are not? There are two reasons: a low electron temperature  $T_e$  and an enhanced N/O ratio. At first, the electron temperature  $T_e$  must be so low that the  $[O II]$  lines are not excited and below the detection limit. We have modelled the  $H II$  region created by  $\alpha$  Sco B in the wind of the M supergiant using the Cloudy code (version 07.02.00, last described by Ferland et al., 1998). Since the B star, with an effective temperature of 18200 K, is relatively cool, the resulting electron temperature is below 5000 K which does not allow  $[O III]$  to exist and predicts  $[O II]/H\alpha$  below our detection limit. But the same model would also predict  $[N II]$  below our detection limit! The solution to this problem is that Antares must have CNO-processed material in its atmosphere and wind. Indeed, it has been shown by Harris & Lambert (1984) that in the atmosphere of Antares  $^{13}C$  and  $^{17}O$  are enhanced, a clear indication of CNO cycle material. Unfortunately there is no direct measurement of the N abundance (or N/O). Typical values for the N enhancement in M supergiants of comparable luminos-

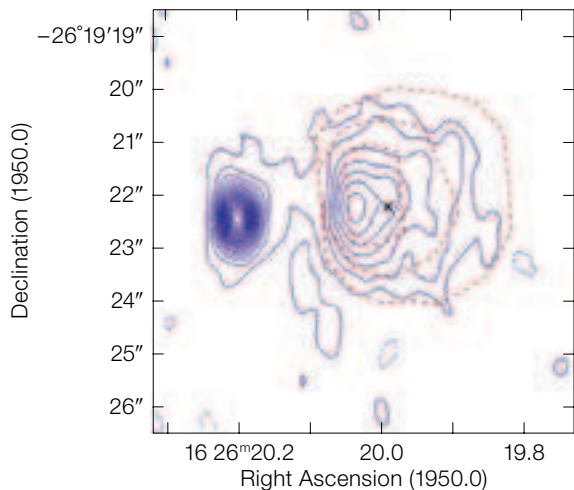


**Figure 4.** Comparison of the distribution of  $H\alpha$  emission with radio free-free emission (Hjellming & Newell, 1983) (blue). Dashed red lines represent half, fourth, and tenth of the central  $H\alpha$  emission flux.

ity are  $[N/H] = 0.6$  (logarithmic abundance ratio relative to solar), while oxygen is slightly reduced,  $[O/H] = -0.1$ . Our best value for the nitrogen abundance determined independently from a fit of the Cloudy models to observed  $[N_{II}]/H\alpha$  values is  $[N/H] = 0.52 \pm 0.1$  with  $[O/H] \leq -0.05$  which is fully consistent with the expectations.

Last but not least: the same Cloudy models with the above mentioned abundances show that metal line cooling of the  $H_{II}$  region is dominated by  $[N_{II}]$  and collisionally excited  $[Fe_{II}]$ . This is at least part of the explanation for the strong  $[Fe_{II}]$  spectrum of the Antares nebula.

### [\[FeII\] emission](#)

The comparison of the distribution of the  $[Fe_{II}]$  emission in position and velocity space with  $H\alpha$  (Figures 2 and 3) shows distinct differences:

- The  $[Fe_{II}]$  emission is not smoothly distributed like  $H\alpha$  and  $[N_{II}]$  but is apparently concentrated on the edges – the ionisation shock fronts – of the  $H_{II}$  region. The  $[Fe_{II}]$  emission thus gives rise to a ring-like structure (extending up to  $\sim 6''$  from Antares outside the  $H_{II}$  region itself), which ends roughly at  $6''$ , thus making a double structure. This ring-like and double-peak shape are apparent from the front and rear side of the  $H_{II}$  region respectively, where the red component (rear side) is always stronger. We notice in passing that the occurrence of  $[Fe_{II}]$  in the Orion Nebula

has also been observed close to the ionisation front (Bautista et al., 1994).

- In addition to emission from the ionisation fronts there is apparently a further component (cf. Figure 3, 4'' to 6'' offset) in the centre of the  $H_{II}$  region. This is again consistent with our Cloudy simulations which show such a further maximum. We notice, however, that the 'central'  $[Fe_{II}]$  emission varies strongly with slit position which may have its origin in a time-variable (episodic) supergiant wind. There is independent evidence, from both IR interferometric imaging of the immediate surrounding of Antares and from the multiple component structure of CS absorption lines seen in HST spectra of  $\alpha$  Sco B (Baade & Reimers, 2007), for a time-variable wind.

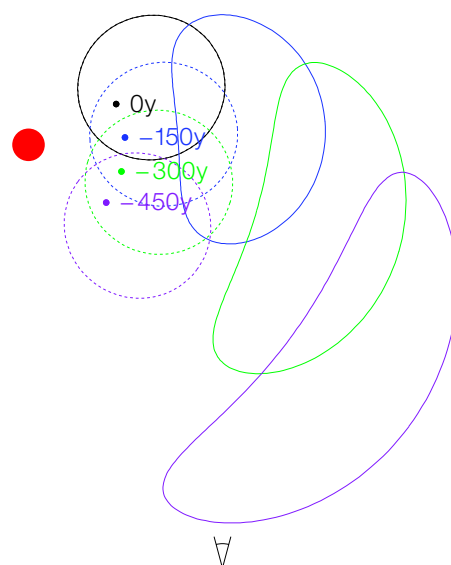
- Emission is clearly seen outside of the  $H_{II}$  region: beyond  $5.9''$  west of A, the  $[Fe_{II}]$  emission becomes more extended and more structured. In velocity space the  $[Fe_{II}]$  emission moves in the mean from  $4 \text{ km s}^{-1}$   $1.9''$  west of A through  $3 \text{ km s}^{-1}$  at B to  $0 \text{ km s}^{-1}$   $5.9''$  west of A and  $\sim -5.5 \text{ km s}^{-1}$  at  $9.9''$  west of A.

Apparently we start to see here time-dependent effects: the M supergiant wind carries the structure imprinted by the  $H_{II}$  region ('shock fronts') to large distances from the system outside the  $H_{II}$  region, where hydrogen is again neutral. In addition, the systematic shift in velocity can be explained by a combination of B star orbital motion with wind expansion. An analysis of the orbit

shows that at present the B star moves nearly perpendicularly into the plane of the sky (Reimers et al., 2008) which, combined with wind expansion, produces a cometary structure (cf. Figure 5).

- The UVES observations with  $45^\circ$  slit position (Figure 1) confirm what Swings & Preston (1978) had seen, namely that faint  $[Fe_{II}]$  emission is seen all along the slit, i.e. in the neutral M star wind. The explanation comes from the observation that one of the allowed lines,  $Fe_{II}$   $5169 \text{ \AA}$ , appears both in the neutral wind (position  $0.9''$  from the M star) and in the  $H_{II}$  region. Apparently one channel for the excitation of the forbidden  $[Fe_{II}]$  lines is line scattering of B star photons in the strong UV resonance lines, which was first seen with IUE (Hagen et al., 1987). One of the strong UV resonance (scattering) lines in the UV spectrum of  $\alpha$  Sco B is the  $Fe_{II}$  UV mult. 3 line at  $2344 \text{ \AA}$ , which shows a P Cyg type profile. In the case of the  $2344 \text{ \AA}$  line, a second downward channel exists via the  $Fe_{II}$  lines  $4923$ ,  $5018$ , and  $5169 \text{ \AA}$  so that part of the

**Figure 5.** 'Look back' contours (solid lines) of  $H_{II}$  region borders in a plane perpendicular to the plane of the sky caused by the combination of wind expansion with orbital motion of  $\alpha$  Sco B relative to  $\alpha$  Sco A. Contours are shown for present and previous phases ( $-150$  yrs to  $-450$  yrs; 150 years being the wind travel time for the projected distance between A and B). This is a qualitative model for the cometary-like structure of the  $[Fe_{II}]$  emission regions.



downward cascade is via these lines and this is what we observe – FeII 5169 Å in emission. This channel populates the upper level of the strongest [FeII] lines 4287 Å and 4359 Å. In conclusion, we have identified in detail from IUE and UVES observations the [FeII] excitation mechanism in the cold, neutral M star wind far outside the HII region.

### Mass loss of $\alpha$ Sco A

The number of Lyman continuum photons and the wind density (mass-loss rate) determine the shape (size) of the HII region. At this time we have performed only static HII region model calculations assuming that the density structure is not grossly disturbed by the

HII region shock fronts – which is certainly an oversimplification. The geometry, i.e. the location of the B star and its HII region relative to the plane of the sky at the M supergiant, has been determined using the H $\alpha$  and [FeII] velocities as 23° behind the plane of the sky.

The best match of the Cloudy models with the observed H $\alpha$  intensity distribution (Figures 2 and 4) yields a mass-loss rate of  $1.05 \times 10^{-6} M_{\odot}/\text{yr}$  with an uncertainty of  $\pm 30\%$ . This is a mean value over the crossing time of the wind through the HII region of roughly 150 yrs. We believe that the new value for the mass-loss rate is more reliable than (our own) previous measurements, mainly because the use of circumstellar absorption lines in the B star spectrum, formed in the vast circumstellar envelope of the M supergiant, suf-

fers from the episodic nature of mass loss (multicomponent absorption) and from the observation that dust depletion onto grains is important (Baade & Reimers, 2007).

### References

- Baade, R. & Reimers, D. 2007, *A&A*, 474, 229  
 Bautista, M. A., Pradhan, A. K. & Osterbrock, D. E. 1994, *ApJ*, 432, L135  
 Ferland, G. J., Korista, K. T., Verner, D. A., et al. 1998, *PASP*, 110, 761  
 Hagen, H.-J., Hempe, K. & Reimers, D. 1987, *A&A*, 184, 256  
 Harris, M. J. & Lambert, D. L. 1984, *ApJ*, 281, 739  
 Hjellming, R. M. & Newell, R. T. 1983, *ApJ*, 275, 704  
 Kudritzki, R. & Reimers, D. 1978, *A&A*, 70, 227  
 Reimers, D., Hagen, H.-J., Baade, R., et al. 2008, *A&A*, submitted  
 Struve, O. & Zeberg, V. 1962, *Astronomy of the 20th Century*, (New York: MacMillan Comp.), 303  
 Swings, J. P. & Preston, G. W. 1978, *ApJ*, 220, 883



Another early VLT image showing the high ionisation bipolar planetary nebula NGC 6302. This colour picture is a composite of three VLT UT1 Test Camera exposures through *B*, *V* and *R* filters, taken in June 1998. The extremely hot ( $\sim 200\,000$  K) central star is hidden within the slender wisp of dust at the core of the nebula.